

conducting magnet, giving rise to a magnetic field (B_{ex}) up to ≈ 4 T at the sample (ME absorber) and zero magnetic field at the $^{57}\text{Co}:\text{Rh}$ source at a distance of ≈ 40 mm from the absorber. The direction of B_{ex} was parallel to the γ -ray direction. Absorber temperature could be varied between 4.2 K and ≈ 100 K; source temperature was kept constant at ≈ 4.2 K. ^{57}Fe ME spectra were taken at various values of B_{ex} (0, 1, 2, and 3 T) for temperatures in the interval $4.2 \leq T \leq 80$ K.

Figure 2 shows the ME spectra at 4.2 K for $B_{ex} = 0, 1, 2,$ and 3 T. The zero-field spectrum shows the well-known six-line Zeeman pattern with a line intensity ratio of 3:2:1:1:2:3, typical for a magnetically ordered sample with randomly distributed spin directions. This line intensity ratio changes drastically by application of B_{ex} as can be seen in Fig. 2. The nonzero intensity of the second and fifth Zeeman line is an indication for the so-called spin canting in the RSG state below T_f .²¹ For spins with their direction parallel to B_{ex} , i.e., parallel to the γ direction, these lines should have zero intensity (line intensity ratio 3:0:1:1:0:3). Figure 3 shows typical ME spectra with $B_{ex} = 3$ T and at various temperatures. The increase of the intensity of the second and fifth line with decreasing temperature ($T < T_f$) is obvious. At higher temperatures ($T_f < T < T_c$) these lines disappear as it should be for an FM ordered sample. In order to get a reliable least-squares fit to these ME spectra, several assumptions have to be made which will be discussed in detail in the next section.

III. PRINCIPLE OF ME SPECTRA ANALYSIS WITHIN THE CANTING MODEL

The information one wants to extract from the ME spectra is the temperature dependence of both the mean

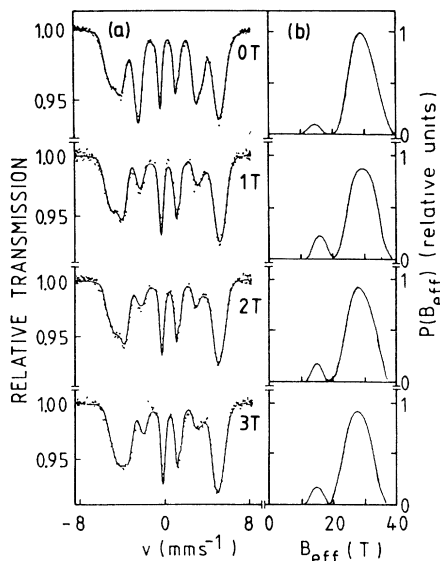


FIG. 2. (a) ^{57}Fe ME spectra of $\text{Au}_{0.832}\text{Fe}_{0.168}$ at 4.2 K for $B_{ex} = 0, 1, 2,$ and 3 T. The lines through the data points are least-squares fits. (b) Magnetic hyperfine field distributions as obtained from least-squares fits of the ME spectra shown in (a).

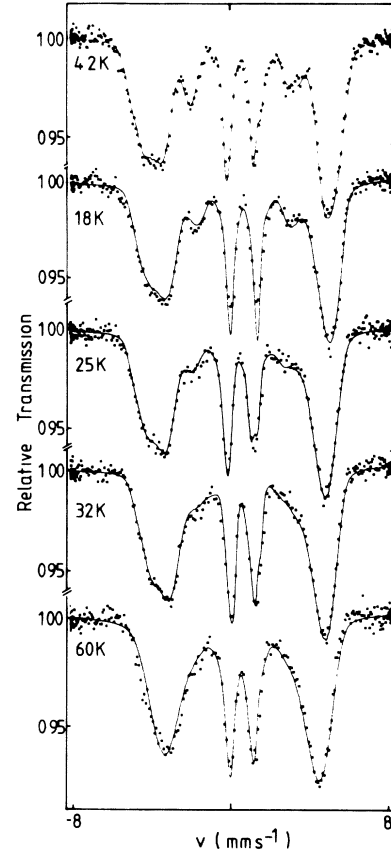


FIG. 3. ^{57}Fe ME spectra of $\text{Au}_{0.832}\text{Fe}_{0.168}$ for $B_{ex} = 3$ T at various temperatures.

effective magnetic hyperfine (hf) field at the ^{57}Fe nucleus, $\langle B_{eff}(T) \rangle$, and the mean canting angle $\langle \theta(T) \rangle$ as a function of B_{ex} . The canting angle θ is defined in Fig. 4 which shows the vector diagram for the RSG state. With the knowledge of $\langle B_{eff}(T) \rangle$ and $\langle \theta(T) \rangle$ for the various values of B_{ex} one can determine the B_{ex} dependence of the reentrance temperature T_f which is defined as that temperature where the spin canting goes to zero, i.e., where both the anomaly in $\langle B_{eff}(T) \rangle$ and the mean canting angle $\langle \theta \rangle$ disappear.¹⁷ $\langle B_{eff} \rangle$ is obtained by fitting the ME spectra with a modified histogram method²⁴ giving the magnetic hf field distribution $P(B_{eff})$ and thus

$$\langle B_{eff} \rangle = \int_0^{(B_{eff})_{max}} P(B_{eff}) B_{eff} dB_{eff}. \quad (1)$$

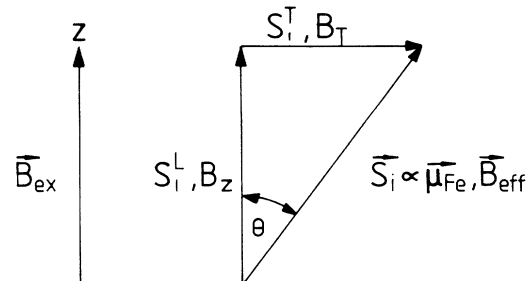


FIG. 4. Vector diagram for spins components (S_i, S_i^L, S_i^T) and magnetic hf field components (B_{eff}, B_z, B_T) in the RSG state.

The mean canting angle $\langle \theta \rangle$, on the other hand, can be obtained from the intensity ratio D_{23} of the second and third Zeeman line in the magnetically split ME spectrum:²⁵

$$D_{23} = 4 \left[\frac{1 - \langle \cos^2 \theta \rangle_{\langle \theta \rangle}}{1 + \langle \cos^2 \theta \rangle_{\langle \theta \rangle}} \right]. \quad (2)$$

$\langle \rangle_{\langle \theta \rangle}$ means an average over the distribution $P(\theta)$ of the canting angle θ with a mean value $\langle \theta \rangle$.

The problem which arises now is the following: $P(B_{\text{eff}})$ and D_{23} cannot be determined unambiguously from the measured ME spectra. This becomes obvious from the ME spectra shown in Figs. 2 and 3: Due to overlapping of the individual Zeeman lines, D_{23} considerably depends on the shape of $P(B_{\text{eff}})$, especially if $P(B_{\text{eff}})$ has a low-field shoulder. This is a well-known problem in ME spectroscopy, for example, also showing up in the ME spectra of metallic glasses.²⁶ A possibility to solve this problem has been proposed by Vincze and Babić.²⁷ We have decided to solve that problem in such a way that the correct solution obtained from the fitting procedure is consistent within the canting model. This is shown in the following.

The mean effective hf field $\langle B_{\text{eff}} \rangle$ in the canting model is connected with the canting angle θ by the following relation:²⁸

$$\langle B_{\text{eff}} \rangle = \langle B_Z \rangle \langle \cos^{-1} \theta \rangle_{\langle \theta \rangle}. \quad (3)$$

$\langle \rangle_{\langle \theta \rangle}$ again means the averaging over the distribution $P(\theta)$ of the canting angle θ with a mean value $\langle \theta \rangle$. This relation follows directly from the vector diagram in Fig. 4. $\langle B_Z \rangle$ in the RSG state can be obtained from $\langle B_{\text{eff}} \rangle$ in the FM state [$T > T_f$: $\langle B_Z(T) \rangle = \langle B_{\text{eff}}(T) \rangle$ for $\theta = 0$] by extrapolation to $T < T_f$ assuming a $T^{3/2}$ -law: $\langle B_Z(T) \rangle = \langle B_Z(0) \rangle [1 - AT^{3/2}]$. Comparing Eqs. (2) and (3) it is obvious that $\langle B_{\text{eff}} \rangle$ and D_{23} are related to each other via the canting angle θ . However, in order to get the $\langle B_{\text{eff}} \rangle$ - D_{23} relation from Eqs. (2) and (3) one has to know the canting-angle distribution $P(\theta)$ for a given mean canting angle $\langle \theta \rangle$. Taking into account that the experimental observed shape of $P(\theta)$ (Ref. 29) has a maximum at $\theta = 0$, a width which is a measure of $\langle \theta \rangle$ and which goes to zero at an upper limit θ_0 , we have approximated $P(\theta)$ by the following function:

$$P(\theta) = \begin{cases} \cos^2(\pi\theta/2\theta_0) & \text{for } \theta \leq \theta_0 \\ 0 & \text{for } \theta \geq \theta_0 \end{cases}. \quad (4a)$$

θ_0 is related to the mean value $\langle \theta \rangle$ by

$$\langle \theta \rangle = \int_0^{\theta_0} \sin\theta P(\theta) \theta d\theta. \quad (4b)$$

The mean value of a θ -dependent quantity $f(\theta)$ can now be calculated with the help of the above given $P(\theta)$ for a given $\langle \theta \rangle$:

$$\langle f(\theta) \rangle_{\langle \theta \rangle} = \frac{\int_0^{\theta_0} \sin\theta P(\theta) f(\theta) d\theta}{\int_0^{\theta_0} \sin\theta P(\theta) d\theta}. \quad (5)$$

We have plotted in Fig. 5 as an example the theoretical

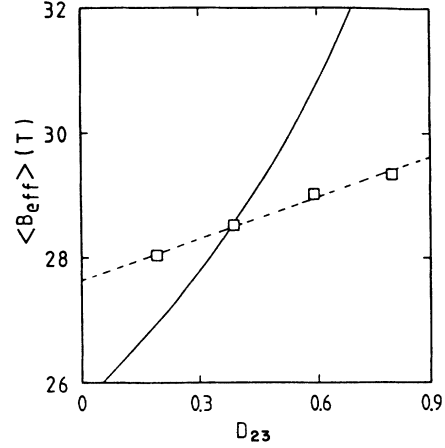


FIG. 5. Connection between D_{23} and $\langle B_{\text{eff}} \rangle$ for $B_{\text{ex}} = 1$ T and $T = 4.2$ K. Solid line: Theoretical curve as obtained from the canting model. Squares (connected by dashed line): Possible solutions of different least-squares fits to the ME spectra. The intersection point is the correct solution within the canting model.

expected $\langle B_{\text{eff}} \rangle$ - D_{23} relation (solid line) for the ME spectrum at $T = 4.2$ K and $B_{\text{ex}} = 1$ T. It was obtained from Eqs. (2)–(5) together with the $\langle B_{\text{eff}}(T) \rangle$ values in the FM state ($T > T_f$). In addition, we have plotted in Fig. 5 the $\langle B_{\text{eff}} \rangle$ values (squares) obtained from different least-squares fits to the ME spectrum at $T = 4.2$ K and $B_{\text{ex}} = 1$ T by assuming different D_{23} values. The least-squares sums essentially have the same value for all of these fits (differences $\lesssim 10\%$). The intersection between the dashed line, which connects the possible fitting solutions,

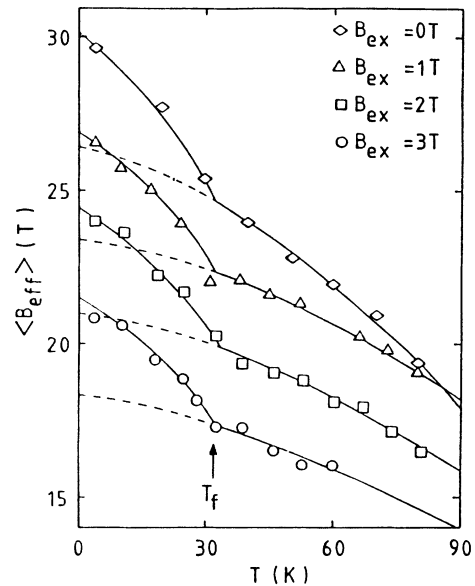


FIG. 6. Temperature dependence of mean hf field $\langle B_{\text{eff}} \rangle$ for $B_{\text{ex}} = 0, 1, 2,$ and 3 T. The curves are shifted by $2B_{\text{ex}}$ downwards in order to prevent overlap of the curves. Thus, the correct hf field values are obtained by adding $2B_{\text{ex}}$ to the given values.

and the theoretical $\langle B_{\text{eff}} \rangle - D_{23}$ relation (solid line) is the *only* solution which is consistent within the canting model.

All ME spectra with $B_{\text{ex}} \neq 0$ in the temperature region $T < T_f$ have been analyzed using the fitting procedure as described above. The spectra for $T > T_f$ (FM state) and $B_{\text{ex}} \neq 0$ have been fitted with $D_{23} = 0$ (spin direction parallel to γ -ray direction), whereas the spectra for $B_{\text{ex}} = 0$ at *all* temperatures have been fitted with $D_{23} = 2$, typical for randomly distributed spin directions. More details of the fitting procedure, e.g., inclusion of quadrupole interaction, are given in Ref. 24. The lines through the data points in Figs. 2 and 3 are least-squares fits obtained in the way described above.

IV. RESULTS

The magnetic hf field distributions $P(B_{\text{eff}})$ for $\text{Au}_{0.832}\text{Fe}_{0.168}$ at 4.2 K in zero field and for $B_{\text{ex}} = 1, 2,$ and 3 T as obtained from least-squares fits to the ME spectra in Fig. 2(a) are displayed in Fig. 2(b). Comparing the different hf field distributions for $B_{\text{ex}} = 0, 1, 2,$ and 3 T it becomes clear that B_{ex} does not change $P(B_{\text{eff}})$ in external fields up to 3 T. This finding is in agreement with the results reported by Whittle *et al.*,³⁰ where no change in $P(B_{\text{eff}})$ with external field $B_{\text{ex}} = 5$ T has been observed in $\text{Au}_{1-x}\text{Fe}_x$ for $x = 0.2$ (RSG state).

Figure 6 shows the temperature dependence of $\langle B_{\text{eff}} \rangle$ for $B_{\text{ex}} = 0, 1, 2,$ and 3 T. The lines through the data points have been obtained in the following way: We have assumed that above the reentrant transition (FM state) $\langle B_{\text{eff}}(T) \rangle$ is described, as already mentioned, by the well-known $T^{3/2}$ law for spin wave excitations. For $T < T_f$ the data points have been fitted by a curve which is based on a Landau expansion for spin glasses,^{31,32} taking into account that the SG order parameter $q = [\langle S_i \rangle]^2$ is replaced by the transversal order parameter $q_T = [\langle S_i^T \rangle]^2$ for the RSG state ($\langle \rangle$ means thermal averaging and $[\]_J$ the average over a Gaussian distribution of bonds J_{ij}). In this case, the transversal component of the effective hf field, B_T , which is proportional to S_i^T (see Fig. 4), can be approximated by

$$B_T(T) = B_T(0)(1 - T/T_f)^\beta. \quad (6)$$

The exponent which gives the best fit of the data is $\beta = 0.4$, somewhat smaller than the mean-field exponent $\beta(\text{MFT}) = 0.5$.

The transition from the FM state to the RSG state at T_f is clearly seen in Fig. 6: A sudden enhancement of the magnitude of $\langle B_{\text{eff}}(T) \rangle$, caused by the additional ordering of S_i^T , occurs at $T_f = 32.5 \pm 2$ K. However, an external magnetic field B_{ex} seems to have no influence on T_f itself ($|\Delta T_f| \lesssim 2$ K for $B_{\text{ex}} = 3$ T). This fact can be even better seen in Fig. 7 where the temperature dependence of the mean canting angle $\langle \theta \rangle$ is plotted for $B_{\text{ex}} = 0, 1, 2,$ and 3 T. The line through the data points is a fit using the approximation described above for $B_T(T)$ [see Eq. (6)] and the relation

$$\langle B_T \rangle = B_Z \langle \tan \theta \rangle_{\langle \theta \rangle}, \quad (7)$$

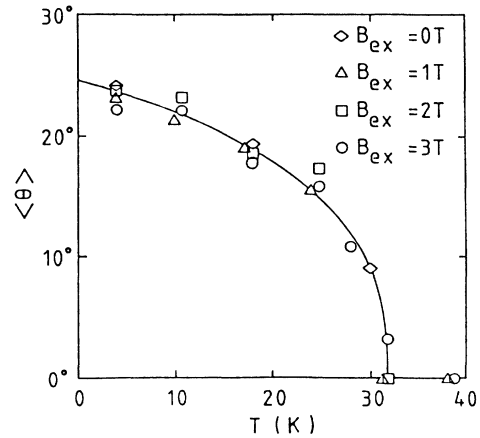


FIG. 7. Temperature dependence of the mean canting angle $\langle \theta \rangle$ for $B_{\text{ex}} = 0, 1, 2,$ and 3 T.

which directly follows from Fig. 4. We can conclude from Fig. 7 that not only T_f but also $\langle \theta(T) \rangle$ does not change with external magnetic field up to 3 T ($\langle \theta(0) \rangle = 25 \pm 1.5^\circ$, $|\Delta \langle \theta(B_{\text{ex}}) \rangle| \lesssim 1.5^\circ$ for $B_{\text{ex}} = 3$ T).^{33,34}

V. DISCUSSION

The most important information we obtain from the ME spectra analysis is the fact that the reentrant temperature T_f does not change with B_{ex} ($|\Delta T_f| \lesssim 2$ K). Our finding is in agreement with the very recent result of Meyer *et al.*³⁵ who studied the influence of an external magnetic field up to 8 T on the reentrant ferromagnet $\text{Au}_{0.81}\text{Fe}_{0.19}$ doped with 2% ^{119}Sn : No change of T_f was observed in these experiments.

In the following we will compare our result on $T_f(B_{\text{ex}})$ with the theoretical predictions by Dubiel *et al.*²⁰ According to this work,

$$\begin{aligned} \Delta T_f &= T_f(B_{\text{ex}}) - T_f(0) \\ &= -2\sqrt{2} \left[\frac{m^2 + 4m + 2}{4(m+2)^2} \right] \left[\frac{g\mu_B}{k_B} \right] B_{\text{ex}}, \end{aligned} \quad (8)$$

which results for $m = 3$ ($m = \text{number of spin components}$) in $\Delta T_f = -2.6$ K for $B_{\text{ex}} = 3$ T.

Our finding of $|\Delta T_f(B_{\text{ex}} = 3 \text{ T})| \lesssim 2$ K, thus, is not quite in contradiction to the mean-field-theory (MFT) result.²⁰ It is, however, in strong disagreement with the $\Delta T_f(B_{\text{ex}})$ results obtained in some other Fe-based RSG systems, where the spin canting has been established by means of ^{57}Fe ME spectroscopy. We have summarized in Table I the existing experimental data on $\Delta T_f(B_{\text{ex}})$ for those RSG systems. According to this table there are two systems where no change in T_f with B_{ex} has been observed ($\text{Au}_{0.832}\text{Fe}_{0.168}$, $\text{Fe}_6\text{Ni}_{72}\text{Si}_9\text{B}_{13}$); two other systems $\text{Cr}_{75}\text{Fe}_{25}$, $(\text{Fe}_{0.65}\text{Ni}_{0.35})_{0.898}\text{Mn}_{0.102}$ show a change in T_f which is large compared to the MFT result. In principle, the MFT result is only valid for the triple point in the magnetic phase diagram (see Fig. 1), i.e., $T_c = T_f(0)$. The

TABLE I. FM ordering temperature (T_c), reentrant temperature for $B_{\text{ex}}=0$ [$T_f(0)$], and the B_{ex} -induced shift ΔT_f of $T_f(0)$ for different Fe-based RSG systems in which the spin canting has been observed by means of ^{57}Fe ME spectroscopy. The theoretical (MFT) result is given for comparison.

	T_c	$T_f(0)$	$\frac{T_c - T_f(0)}{T_f(0)}$	$-\Delta T_f / B_{\text{ex}}$	Ref.
	(K)	(K)		(K/T)	
Theory (MFT)				0.87	20
$\text{Au}_{0.832}\text{Fe}_{0.168}$	165	33	≈ 4	$\lesssim 0.7$	This work
$\text{Fe}_6\text{Ni}_{72}\text{Si}_9\text{B}_{13}$	45	13	≈ 3	≈ 0	37
$\text{Cr}_{75}\text{Fe}_{25}$	160	30	≈ 4	6.0 ± 1.0	20
$(\text{Fe}_{0.65}\text{Ni}_{0.35})_{0.898}\text{Mn}_{0.102}$	230	38	≈ 5	≈ 12	38
				(for $B_{\text{ex}} \lesssim 0.5$ T)	

measurements, on the other hand, have all been made in the RSG state for concentrations where $T_c > T_f(0)$. The fourth column in Table I gives the ratio $[T_c - T_f(0)]/T_f(0)$ which, as we think, can be taken as a measure of the degree of deviation from the triple point. These ratios essentially have the same order of magnitude, i.e., the systems can be compared from that point of view. The only obvious difference between the systems with no (or small) $\Delta T_f(B_{\text{ex}})$ values and those with large $\Delta T_f(B_{\text{ex}})$ values, is the following: The first class of systems contains magnetically diluted FM systems, where the antiferromagnetic (AF) interaction and thus the frustration enters via the *long*-range RKKY interaction, whereas in the second class one has *short*-range, direct AF interaction (introduced by Cr and Mn, respectively).³⁶ This difference in the AF interaction length probably leads to different local spin correlations. In the case of $\text{Au}_{0.832}\text{Fe}_{0.168}$, for example, it was shown^{8,9} that the spin canting in the RSG state is locally correlated, which leads to the picture of canted spin *clusters*. Such canted spin clusters will have a larger stability against external magnetic fields compared to individual canted spins probably present in the second class of systems. Thus, it appears that the different local spin correlations of the RSG state present in different RSG systems are reflected in a different B_{ex} dependence of T_f .

The additional information we obtain from our analysis is that also the mean canting angle $\langle \theta(T) \rangle$ does *not* change with B_{ex} up to 3 T ($|\Delta \langle \theta \rangle| \lesssim 1.5^\circ$, see Fig. 7). This finding, together with the fact that $P(B_{\text{eff}})$ does not change with B_{ex} (see Sec. IV and Ref. 30), leads us to the conclusion that the local spin structure of the RSG state

in the system $\text{Au}_{0.832}\text{Fe}_{0.168}$ is stable against external magnetic fields up to 3 T. On the other hand, we observe that the *FM state* is stabilized by the external magnetic field: The decrease of $B_{\text{eff}}(T)$ for $T > T_f$ is found to be weaker for $B_{\text{ex}} \neq 0$ when compared with that in zero field (see Fig. 6). This finding, again, was also observed in Ref. 35 where it is explained by the presence of cooperative ordered, superparamagnetic clusters in the FM state.

VI. CONCLUSION

External magnetic fields up to $B_{\text{ex}} \approx 3$ T have no measurable influence on the RSG state of $\text{Au}_{0.832}\text{Fe}_{0.168}$: The reentrance temperature T_f as well as the mean canting angle $\langle \theta \rangle$ do not change with B_{ex} . This result, while not in contradiction to an existing MFT result, is quite different from that observed in some other RSG systems. Thus, we conclude that the local spin structure of the RSG state is quite system dependent. In the case of RSG $\text{Au}_{0.832}\text{Fe}_{0.168}$ the local spin structure shows ferromagnetic correlations, which may be responsible for the high stability of this RSG state upon application of an external magnetic field.

ACKNOWLEDGMENTS

This work was supported by the Deutsche Forschungsgemeinschaft (Sonderforschungsbereich No. 166). Helpful discussions with J. Hesse and W. Keune are gratefully acknowledged.

¹B. R. Coles, B. V. B. Sarkissian, and R. M. Taylor, Philos. Mag. **37B**, 489 (1978).

²B. H. Verbeek and J. A. Mydosh, J. Phys. F **8**, L109 (1978).

³M. Gabay and G. Toulouse, Phys. Rev. Lett. **47**, 201 (1981).

⁴C. E. Violet and R. J. Borg, Phys. Rev. Lett. **51**, 1073 (1983).

⁵P. A. Beck, Phys. Rev. B **32**, 7255 (1983).

⁶M. Avirovic and P. Ziemann, Europhys. Lett. **8**(3), 278 (1989).

⁷D. Boumazouza, P. H. Mangin, B. Georg, P. Louis, R. A. Brand, J. J. Rhyne, and R. W. Erwin, Phys. Rev. B **39**, 749 (1989).

⁸M. M. Abd-Elmeguid, H. Micklitz, R. A. Brand, and W. Keune, Phys. Rev. B **33**, 7833 (1986).

⁹A. Ait-Bahammou, C. Meyer, F. Hartmann-Boutron, Y. Gros, and I. A. Campbell, J. Phys. (Paris) Colloq. **49**, C8-1157

- (1988).
- ¹⁰J. R. L. de Almeida and D. J. Thouless, *J. Phys. A* **11**, 983 (1978).
- ¹¹P. Monod and H. Bouchiat, *J. Phys. Lett. (Paris)* **43**, L45 (1982).
- ¹²A. P. Malozemoff, S. E. Barnes, and B. Barbara, *Phys. Rev. Lett.* **51**, 1704 (1983).
- ¹³A. C. Palumbo, R. D. Parks, and Y. Yeshurn, *J. Magn. Magn. Mater.* **36**, 66 (1983).
- ¹⁴I. A. Campbell, N. de Courtenay, and A. Fert, *J. Phys. Lett. (Paris)* **45**, L565 (1984).
- ¹⁵B. Barbara, A. P. Malozemoff, and S. E. Barnes, *J. Appl. Phys.* **55**, 1655 (1984).
- ¹⁶C. Paulsen, J. A. Hamida, S. J. Williamson, and H. Maletta, *J. Appl. Phys.* **55**, 1652 (1984).
- ¹⁷M. Rots, L. Hermans, and J. van Canteren, *Phys. Rev. B* **30**, 3666 (1984).
- ¹⁸G. A. Takzei, A. M. Kastyshin, and Yu. P. Grebenyuk, *Fiz. Tverd. Tela (Leningrad)* **26**, 2722 (1984) [*Sov. Phys.—Solid State* **26**, 1648 (1984)].
- ¹⁹R. V. Chamberlin, M. Hardiman, L. A. Turkevich, and R. Orbach, *Phys. Rev. B* **25**, 6720 (1982).
- ²⁰S. M. Dubiel, K. H. Fischer, Ch. Sauer, and W. Zinn, *Phys. Rev. B* **36**, 360 (1978).
- ²¹J. Lauer and W. Keune, *Phys. Rev. Lett.* **48**, 1850 (1982).
- ²²F. Varret, A. Hamzić, and I. A. Campbell, *Phys. Rev. B* **26**, 5195 (1982).
- ²³R. A. Brand, J. Lauer, and W. Keune, *Phys. Rev. B* **31**, 1630 (1985).
- ²⁴R. A. Brand, J. Lauer, and D. M. Herlach, *J. Phys. F* **13**, 675 (1983).
- ²⁵See, e.g., G. K. Wertheim, *Mössbauer Effect: Principles and Applications* (Academic, New York, 1964).
- ²⁶A. S. Schaafsma, *Phys. Rev. B* **23**, 4784 (1981).
- ²⁷I. Vincze and E. Babić, *Solid State Commun.* **27**, 1425 (1978).
- ²⁸It should be mentioned that $\langle \cos^{-1}\theta \rangle_{\langle \theta \rangle} \simeq (\langle \cos\theta \rangle_{\langle \theta \rangle})^{-1}$, i.e., that it does not matter if we take S and $\cos^{-1}\theta$ or S_z and $\cos\theta$ as the intrinsic statistical variables. In the former case we get formula (3) as given below, while in the latter case formula (3) would read $\langle B_z \rangle = \langle B_{\text{eff}} \rangle \langle \cos\theta \rangle_{\langle \theta \rangle}$. The latter formula is more consistent with the canting model at $T=0$ K where the total spin S has a fixed value.
- ²⁹R. A. Brand, *Nucl. Instrum. Methods Phys. Res.* **28B**, 417 (1978).
- ³⁰G. L. Whittle, S. J. Campbell, and B. D. Maquire, *Hyperfine Interact.* **15/16**, 661 (1983).
- ³¹M. Suzuki, *Prog. Theor. Phys.* **58**, 1151 (1977).
- ³²S. E. Barnes, A. P. Malozemoff, and B. Barbara, *Phys. Rev. B* **30**, 2765 (1984).
- ³³This finding is in contrast to that reported in Refs. 21 and 34. There, however, the detailed analysis of the ME spectra, as described in Sec. III, has not been performed.
- ³⁴R. A. Brand, V. Manns, and W. Keune, *Heidelberg Colloquium on Spinglasses*, Vol. 192 of *Lecture Notes in Physics* (Springer, Berlin, 1983), p.79.
- ³⁵C. Meyer, F. Hartmann-Boutron, J. M. Greneche, and F. Varret, *J. Phys. (Paris) Colloq.* **49**, C8-1155 (1988).
- ³⁶As a consequence of this, the magnetic phase diagram in the second class of systems shows an AF phase at the Cr- and Mn-rich side, respectively, whereas such a phase is missing in the first class of systems.
- ³⁷V. Manns, R. A. Brand, W. Keune, and R. Marx, *Solid State Commun.* **48**, 811 (1983).
- ³⁸K. Mausbach, M. M. Abd-Elmeguid, and H. Micklitz (unpublished).